Fluorescent Probes

DOI: 10.1002/ange.201004976

Design of a Highly Sensitive Fluorescent Probe for Interfacial Electron Transfer on a TiO_2 Surface**

Takashi Tachikawa, Nan Wang, Soichiro Yamashita, Shi-Cong Cui, and Tetsuro Majima**

Electron transfer (ET) is a key process in various chemical and biochemical reactions.[1] For example, interfacial ET in nanoscale TiO_2-based systems governs their photocatalytic performance, and thus a proper understanding of the ET mechanism can provide valuable information for designing highly efficient photocatalysts.[2] Fluorescence at the single-molecule or single-particle level has recently evolved as an important tool for studying catalytic reactions on solid surfaces, because of its high sensitivity, simplicity of data collection, and high spatial resolution in microscopic imaging techniques.[3] For instance, several organic dye probes have been successfully employed to detect the generated reactive oxygen species and identify the active sites on individual TiO_2 nanoparticles by utilizing single-molecule fluorescence spectroscopy.[4] Nevertheless, there are very limited single-molecule studies on dyes that respond to the reduction reactions involved in ET; hence, there is a tremendous need to develop new suitable fluorescent probes for exploring ET processes in heterogeneous catalysis.[5]

We have now designed and synthesized a redox-responsive boron dipyrromethane fluorescent probe, namely, 3,4-dinitrophenyl-BODIPY (DN-BODIPY, Figure 1A) on the basis of a photoinduced intramolecular ET mechanism. Both ensemble-averaged and single-molecule fluorescence experiments demonstrated that DN-BODIPY can act as a highly sensitive nanosensor to monitor photoinduced ET process on the TiO_2 surface.

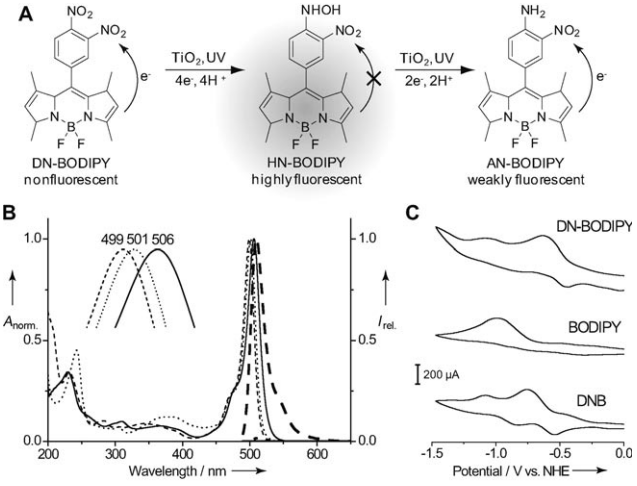

Figure 1. A) Photocatalytic generation of fluorescent HN-BODIPY from nonfluorescent DN-BODIPY. B) Normalized UV/Vis absorption (fine lines) and fluorescence (bold lines, excitation at 470 nm) spectra of DN-BODIPY (solid lines), HN-BODIPY (dashed lines), and AN-BODIPY (dotted lines). The inset shows the magnified absorption peaks. C) Cyclic voltammograms of 1.0 mM DN-BODIPY, BODIPY, and *o*-dinitrobenzene (DNB) in Ar-saturated anhydrous solutions of electrolytes in acetonitrile.

The dye DN-BODIPY is composed of a fluorescent chromophore (BODIPY core) and a reactive site (dinitrophenyl group). The BODIPYs are of interest as fluorophores due to their attractive properties, such as a high extinction coefficient ε, high fluorescence quantum yield Φ_{fl}, and good chemical and photostability, which facilitate their use in chemical and biosensor applications.[6] On the other hand, reduction of aromatic nitro compounds to the corresponding hydroxylamines or amines is one of the most important transformations in synthetic organic chemistry and biochemistry, and thus has been used as a model system to investigate (photo)catalytic reduction reactions with semiconductor and metal nanoparticles.[7] However, in order to develop a fluorogenic probe for monitoring ET process that exploits the reduction of a nitro-substituted benzene moiety, a major drawback must be overcome: nitrobenzene and its reduction products (i.e., phenylhydroxylamine or aniline) are believed to be strong quenchers of fluorescence dyes.[8] The nitro group greatly lowers the LUMO energy level of the benzene moiety at the *meso* position of the BODIPY core because of its strongly electron withdrawing nature, and thus significant quenching of BODIPY fluorescence occurs by intramolecular ET from the excited fluorophore to the nitro-substituted benzene moiety (donor-excited ET). Oppositely, because the electron-donating hydroxylamino and amino groups greatly

[*] Dr. T. Tachikawa, N. Wang, S. Yamashita, S.-C. Cui, Prof. Dr. T. Majima
The Institute of Scientific and Industrial Research (SANKEN)
Osaka University
Mihogaoka 8-1, Ibaraki, Osaka 567-0047 (Japan)
Fax: (+81) 6-6879-8499
E-mail: tachi45@sanken.osaka-u.ac.jp
majima@sanken.osaka-u.ac.jp
N. Wang
College of Chemistry and Chemical Engineering
Huazhong University of Science and Technology
Wuhan 430074 (P.R. China)

[**] N.W. thanks Prof. Lihua Zhu at Huazhong University of Science and Technology and the CSC (China Scholarship Council) program for support. T.M. thanks the WCU (World Class University) program through the National Research Foundation of Korea funded by the Ministry of Education, Science and Technology (R31-10035) for support. This work was partly supported by a Grant-in-Aid for Scientific Research (Projects 22245022, 21750145, and others) from the Ministry of Education, Culture, Sports, Science and Technology (MEXT) of the Japanese Government.

Supporting information for this article is available on the WWW under http://dx.doi.org/10.1002/anie.201004976.

increase the HOMO energy level of the benzene moiety, the BODIPY fluorescence is quenched by an acceptor-excited ET process (Section S4 of the Supporting Information). Indeed, our preliminary experiments confirmed that a mono-nitro-substituted BODIPY derivative (i.e., 4-nitrophenyl-BODIPY) was a failure as fluorescent probe, although it underwent a similar reduction reaction to DN-BODIPY (Figure S2 in the Supporting Information).

The redox properties of DN-BODIPY were determined by cyclic voltammetry (CV) in acetonitrile. As shown in Figure 1C, DN-BODIPY showed two reversible cathodic waves in the window of 0 to −1.5 V versus normal hydrogen electrode (NHE). Compared to the reference compounds *ortho*-dinitrobenzene (DNB, reactive site) and BODIPY without any substituent at the *meso* position (fluorophore core; Invitrogen, D3921), the first cathodic wave at a half-wave potential ($E_{1/2}$) of −0.54 V versus NHE can be assigned to the reduction of the *para*-nitro group, while the second cathodic wave at an $E_{1/2}$ of −0.98 V versus NHE is likely related to reduction of the BODIPY unit to the corresponding radical anion (BODIPY$^{\bullet-}$).[9] This result suggests that reduction of the second nitro group in DN-BODIPY is difficult, possibly because the produced *para*-hydroxylamino or amino group would increase the electron density of the *meta*-nitro group, which would be unfavorable for successive reduction.[10] It is thus anticipated that the above-mentioned intramolecular ET process is suppressed when the produced electron-donating group encounters the benzene moiety with a nitro group, and a highly fluorescent compound is formed (Scheme S4 and Table S1 in the Supporting Information).

The performance and applicability of our ET probe was first examined by evaluating the photocatalytic reduction of TiO_2 nanoparticles (Ishihara Sangyo A-100, particle size 100–200 nm) by ensemble-averaged spectroscopy. When TiO_2 dispersions containing DN-BODIPY (50 μM, in Ar-saturated methanol) were exposed to 365 nm UV light, a new fluorescence peak appeared at about 510 nm and its intensity dramatically increased with increasing UV irradiation time (Figure 2A). In control experiments, the increase in fluorescence intensity was negligible when the suspension was not irradiated with UV light or no TiO_2 photocatalyst was added to the solution (Figure 2B). Since the photogenerated holes in TiO_2 are efficiently scavenged by methanol,[11] it can be suggested that the photogenerated electrons in TiO_2 are mainly responsible for reduction of DN-BODIPY to generate the fluorescent product.

We carefully separated the fluorescent product by preparative layer chromatography and identified it as 4-hydroxyamino-3-nitrophenyl-BODIPY (HN-BODIPY) using ^{1}H NMR, mass, UV/Vis absorption, and fluorescence (excitation) spectroscopy (see Figure 1B and Section S6 of the Supporting Information). Compared to DN-BODIPY and other possible reduced species, that is, 4-amino-3-nitrophenyl-BODIPY (AN-BODIPY), HN-BODIPY showed a high fluorescence quantum yield and a greatly prolonged fluorescence lifetime (Table 1). The shapes of the fluorescence excitation spectra recorded after UV irradiation were also nearly identical to the absorption spectrum of the purified fluorescent product, and this implies that there was only one

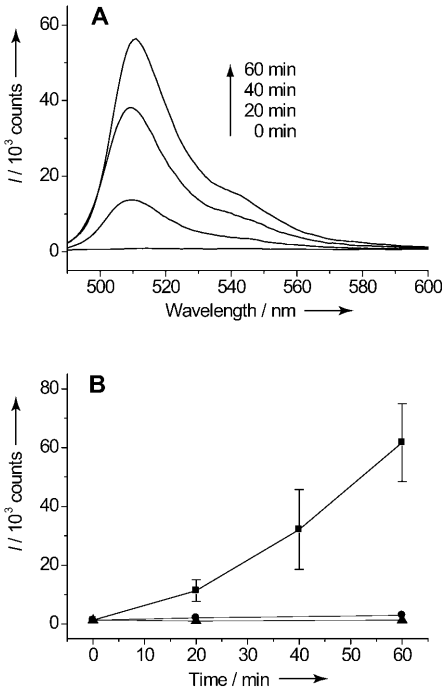

Figure 2. A) Dependence on UV irradiation time of fluorescence spectra of methanol solutions containing DN-BODIPY and TiO_2 particles (excitation at 470 nm). B) Fluorescence intensities measured before and after UV irradiation of the DN-BODIPY solutions with (■) and without (●) TiO_2 or after being placed in the dark with TiO_2 (▲).

Table 1: Photoabsorption and fluorescence properties of BODIPY derivatives in methanol.

Compound	$\lambda_{max,abs}$ [nm]	$\lambda_{max,em}$ [nm]	Φ_{fl}[a]	τ_{fl} [ns]
DN-BODIPY	506	525	0.00011	<0.03
HN-BODIPY	499	510	0.50	3.7
AN-BODIPY	501	512	0.0025	<0.05

[a] Calculated with fluorescein as fluorescence standard ($\Phi_{fl}=0.850$ in 1 N NaOH).

fluorescent product (Figure S3 in the Supporting Information). Based on the above observations, we propose the photocatalytic reduction route of DN-BODIPY over TiO_2 shown in Figure 1A. It is thermodynamically possible that the photogenerated electrons in TiO_2 (conduction band edge energy $E_{CB}=-0.88$ V vs. NHE in methanol)[12] are transferred to DN-BODIPY molecules adsorbed on the TiO_2 surface and lead to the generation of HN-BODIPY. Because the reduction potential of phenylhydroxylamine to aniline is more negative than that of nitrobenzene to phenylhydroxylamine, successive reduction of HN-BODIPY would be minor.[10,13]

We then focused on photocatalytic reduction of DN-BODIPY molecules over single TiO_2 particles by utilizing total internal reflection fluorescence microscopy (TIRFM). Figure 3A shows typical fluorescence images captured for a single TiO_2 particle in Ar-saturated methanol containing DN-BODIPY (2 μM) under UV irradiation (middle and right images). Individual single particles show a number of

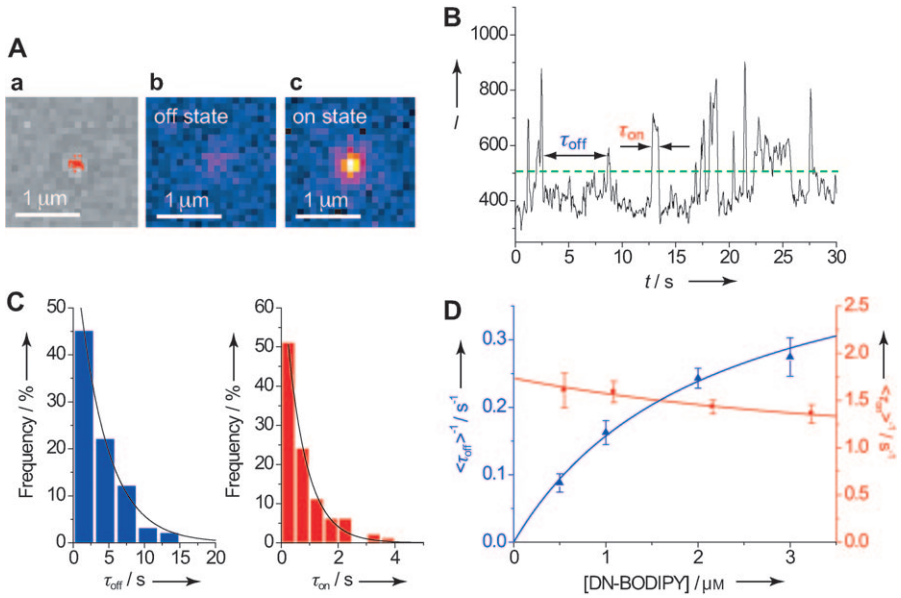

Figure 3. A) Transmission (a) of a single TiO_2 particle on the cover glass and fluorescence images (b, c) of the same particle in Ar-saturated 2.0 μM DN-BODIPY solution under 488 nm laser and UV irradiation (0.5 $W cm^{-2}$ at the glass surface). The acquisition time of an image was 50 ms. The red dots in the transmission image indicate the location of fluorescence bursts. The accuracy of location was about 50 nm. B) A typical fluorescence intensity trajectory observed for a single TiO_2 particle. The green dashed line indicates the threshold level separating the on and off states. C) Off- (blue) and on-time (red) distributions constructed from over 100 events for 20 different single TiO_2 particles. D) Dependence on DN-BODIPY concentration of $\langle\tau_{off}\rangle^{-1}$ (blue) and $\langle\tau_{on}\rangle^{-1}$ (red) obtained for TiO_2. The solid blue and red lines were obtained from Equations (1) and (2), respectively.

fluorescence bursts that have signals over the background (also see Figure 3B). Control experiments also confirmed that TiO_2, DN-BODIPY, and UV excitation are essential for generation of fluorescence bursts. The locations of the fluorescence bursts, which were determined by fitting two-dimensional Gaussian functions to the intensity distribution of each fluorescence spot, are likely distributed over the particle (see the red dots in the transmission image of Figure 3A).[14] Moreover, the fluorescence lifetimes of the in situ generated bursts over single TiO_2 particles were measured by combining confocal microscopy with a time-correlated single-photon counting (TCSPC) system. The fluorescence bursts exhibited a much longer lifetime than the background signal from DN-BODIPY in solution, and thus suggest that such a sudden intensity increase corresponds to generation of the fluorescent product (i.e., HN-BODIPY; Figure S4 in the Supporting Information). Compared to free HN-BODIPY in bulk solution ($\tau_{fl} = 3.7$ ns), these in situ generated products on TiO_2 showed much shorter lifetimes ($\tau_{fl} \approx 1.3$ ns), possibly due to ET from the excited BODIPY chromophore to the TiO_2 nanoparticles (Figure S5 and Table S3 in the Supporting Information).

Accordingly, we could directly evaluate the photocatalytic reduction reactions on individual TiO_2 particles using TIRFM with DN-BODIPY as redox-responsive fluorescent probe. Figure 3B shows a typical fluorescence intensity trajectory obtained for a single TiO_2 particle. In the single-particle turnover trajectory, the actual photocatalytic events can be separated into two characteristic durations τ_{off} and τ_{on}, where τ_{off} is the characteristic time before the formation of fluorescent products on TiO_2, and τ_{on} the characteristic time for which persistent emission is exhibited, which should be related to dissociation of products from the surface rather than their photobleaching or blinking (Figure S6 in the Supporting Information). As depicted in Figure 3C, the distributions of τ_{on} and τ_{off} are well fitted by a single-exponential decay function ($R^2 > 0.97$). Plotting the reciprocals of the average values of τ_{off} ($\langle\tau_{off}\rangle$) and τ_{on} ($\langle\tau_{on}\rangle$) against substrate concentration [**S**] (Figure 3D) reveals that the rate of fluorescent product formation $\langle\tau_{off}\rangle^{-1}$ is dependent on [**S**], as expected. At higher concentrations, a faster adsorption equilibrium is attained which assists reduction of DN-BODIPY to the fluorescent products and leads to an enhancement in $\langle\tau_{off}\rangle^{-1}$.

The dependence of the product formation rate on [**S**] can be described by Langmuir–Hinshelwood equation (1)[15]

$$\langle\tau_{off}\rangle^{-1} = \frac{\gamma_{eff} K_1 [\mathbf{S}]}{1 + K_1 [\mathbf{S}]} \quad (1)$$

where K_1 is the equilibrium adsorption constant for substrate ($K_1 = k_1[\mathbf{S}]/k_{-1}$), and γ_{eff} the reactivity of all catalytic sites ($\gamma_{eff} = k n_s$, where k is the rate constant for one catalytic site, and n_s the total number of substrate binding sites on one particle). The resulting value of K_1 is (0.47 ± 0.10) μM^{-1} for the adsorption of DN-BODIPY on TiO_2 surface, which is of the same order of magnitude as those for nitrobenzenes.[16]

In contrast, the DN-BODIPY concentration has no significant effect on $\langle\tau_{on}\rangle^{-1}$. According to the literature,[15] the main feature of the kinetics of the substrate-assisted product dissociation is described by Equation (2)

$$\langle\tau_{on}\rangle^{-1} = \frac{k_2 K_2 [\mathbf{S}] + k_3}{1 + K_2 [\mathbf{S}]} \quad (2)$$

where k_2 is the rate constant of product dissociation in the substrate-assisted pathway, k_3 the rate constant of direct product dissociation, and $K_2 = k_1/(k_{-1}+k_2)$. By fitting Equation (2) to the data, the k_3 value was determined to be (1.7 ± 0.1) s^{-1}, which is much higher than the k_2 value of (0.33 ± 0.43) s^{-1} (Figure 3D) and thus suggests that the disappearance of HN-BODIPY from the surface of the nanoparticles does not involve the substrate-assisted steps.[17]

Finally, we demonstrate that single-molecule fluorescence imaging with DN-BODIPY allows precise mapping of photocatalytic activity in individual TiO_2 crystals at the nanometer scale (Figure 4). Interestingly, most fluorescence spots were

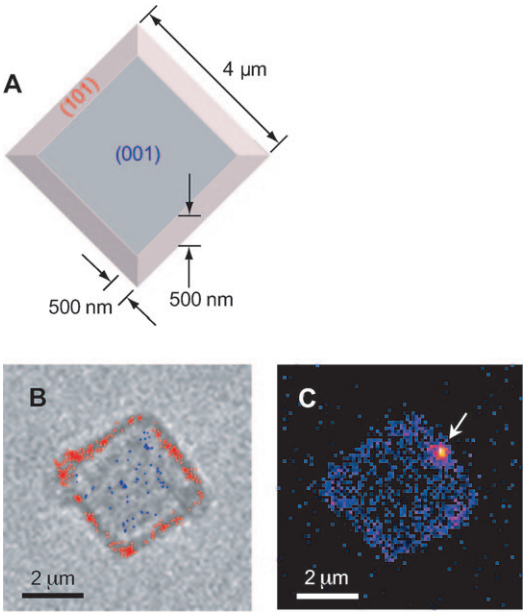

Figure 4. A) Structure of anatase TiO_2 crystal with preferential (001) facets. Transmission (B) of a single TiO_2 crystal on the cover glass and fluorescence (C) images of the same crystal in Ar-saturated 2.0 μM DN-BODIPY solution under 488 nm laser and UV irradiation (30 $mW cm^{-2}$ at the glass surface). The red and blue dots in image B) indicate the fluorescence bursts located on the (101) and (001) surfaces, respectively, observed during 3 min irradiation. The precise positions at which fluorescent products were generated were determined by centroid analysis. The arrow in image C) indicates the fluorescence spot.

found to be preferentially located on the (101) surface of the crystal (see red dots in image B). A similar tendency was observed for more than five individual crystals examined. The average counting rates of single dye molecules were roughly estimated to be (53 ± 10) and (17 ± 4) molecules $\mu m^{-2} min^{-1}$ for (101) and (001) surfaces, respectively; this strongly indicates the effect of crystal facets on the photocatalytic activity, which is not evident in the bulk measurement.[18] Our finding is generally consistent with previous studies and may be explained by differences in surface energy levels of the conduction and valence bands, surface structures, and adsorption energies of substrates on the exposed crystal faces.[19] However, further work is needed to clarify the detailed mechanism of the face-selective photocatalytic reaction.

In conclusion, we propose novel single-molecule fluorescence probe DN-BODIPY for studying the reduction process involved in ET on the TiO_2 surface. Single-molecule kinetic and imaging analyses of the fluorescence bursts emitted from the products revealed the temporal dynamics of molecular interactions and interfacial ET, and heterogeneous distributions of reactive sites on individual catalyst particles. Our methodology should provide a suitable approach to exploring the electron-transport characteristics in various semiconductor (photo)catalysts as well as metal–semiconductor and semiconductor–semiconductor nanocomposites.

Experimental Section

BODIPY derivatives were synthesized according to literature procedures with some modifications (see Supporting Information for details)[20]

Microsized anatase TiO_2 crystals with dominant (001) facets were prepared by the hydrothermal method from titanium sulfate and hydrofluoric acid according to literature procedures (see Supporting Information for details).[21]

Steady-state UV/Vis absorption spectra were measured by a Shimadzu UV-3100 UV/Vis/NIR spectrophotometer. Steady-state fluorescence spectra were measured by a Hitachi 850 or HORIBA FluoroMax-4 fluorescence spectrophotometer. Cyclic voltammetry (CV) measurements were carried out at room temperature with an electrochemical analyzer (ALS, 660A) with a standard three-electrode configuration.

The experimental setup for single-particle experiments was based on an Olympus IX71 inverted fluorescence microscope.[4] The details of the experimental setup are described in the Supporting Information. The position of the TiO_2 particles immobilized on the cover glass was determined from the transmission image obtained by illuminating the sample from above with a halogen lamp (Olympus, U-LH100L-3). Circularly polarized light emitted from a CW Ar ion laser (Melles Griot, IMA101010BOS; 488 nm, 0.1 $kW cm^{-2}$ at the glass surface) was reflected by a first dichroic mirror (Olympus, RDM450) toward a second dichroic mirror (Olympus, DM505). The laser light passing through an objective lens (Olympus, UPLSAPO 100XO; 1.40 NA, 100×) after the reflection at the second dichroic mirror was totally reflected at the cover glass/methanol interface, which generated an evanescent field, making it possible to detect a single fluorescence dye molecule. For excitation of the TiO_2 particles, the 365 nm light emitted by an LED (OPTO-LINE, MS-LED-365) and passing through a neutral density (ND) filter was passed through the objective. The fluorescence emission from the fluorescent products generated over a single TiO_2 particle on the cover glass was collected by using the same objective, magnified by a 1.6× built-in magnification changer, passed through a bandpass filter (Semrock, FF01-531/40-25) to remove the undesired scattered light, and then imaged by an electron-multiplying charge-coupled device (EM-CCD) camera (Roper Scientific, Cascade II:512). The images were recorded at a frame rate of 20 $frames s^{-1}$. All experimental data were obtained at room temperature.

Confocal fluorescence images were taken by using an objective-scanning confocal microscope system (PicoQuant, MicroTime 200) coupled to an Olympus IX71 inverted fluorescence microscope. The samples were excited through an oil-immersion objective lens (Olympus, UAPON 150XOTIRF; 1.45 NA, 150×) with a 485 nm pulsed laser (PicoQuant, LDH-D-C-485; 2 $kW cm^{-2}$ at the glass surface) controlled by a PDL-800B driver (PicoQuant). The emission from the sample was collected by the same objective and detected by a single-photon avalanche photodiode (Micro Photon Devices, PDM 50CT) through a dichroic beam splitter and bandpass filter (Semrock, FF01-531/40-25).

Received: August 10, 2010
Published online: October 4, 2010

Keywords: electron transfer · fluorescent probes · nanoparticles · photochemistry · single-molecule studies

[1] *Electron Transfer in Chemistry*, *Vols. 1–5* (Ed.: A. Balzani), Wiley-VCH, Weinheim, **2001**.
[2] a) M. R. Hoffmann, S. T. Martin, W. Choi, D. W. Bahnemannt, *Chem. Rev.* **1995**, *95*, 69–96; b) T. Tachikawa, M. Fujitsuka, T. Majima, *J. Phys. Chem. C* **2007**, *111*, 5259–5275.

[3] a) M. B. J. Roeffaers, B. F. Sels, H. Uji-i, F. C. De Schryver, P. A. Jacobs, D. E. De Vos, J. Hofkens, *Nature* **2006**, *439*, 572 – 575; b) M. B. J. Roeffaers, G. De Cremer, H. Uji-i, B. Muls, B. F. Sels, P. A. Jacobs, F. C. De Schryver, D. E. De Vos, J. Hofkens, *Proc. Natl. Acad. Sci. USA* **2007**, *104*, 12603 – 12609; c) B. M. Weckhuysen, *Angew. Chem.* **2009**, *121*, 5008 – 5043; *Angew. Chem. Int. Ed.* **2009**, *48*, 4910 – 4943.

[4] T. Tachikawa, T. Majima, *Langmuir* **2009**, *25*, 7791 – 7802.

[5] a) W. Xu, J. S. Kong, Y.-T. E. Yeh, P. Chen, *Nat. Mater.* **2008**, *7*, 992 – 996; b) W. Xu, H. Shen, Y. J. Kim, X. Zhou, G. Liu, J. Park, P. Chen, *Nano Lett.* **2009**, *9*, 3968 – 3973; c) T. Tachikawa, S. Yamashita, T. Majima, *Angew. Chem.* **2010**, *122*, 442 – 445; *Angew. Chem. Int. Ed.* **2010**, *49*, 432 – 435.

[6] A. Loudet, K. Burgess, *Chem. Rev.* **2007**, *107*, 4891 – 4932.

[7] a) J. L. Ferry, W. H. Glaze, *Langmuir* **1998**, *14*, 3551 – 3555; b) A. Corma, P. Concepción, P. Serna, *Angew. Chem.* **2007**, *119*, 7404 – 7407; *Angew. Chem. Int. Ed.* **2007**, *46*, 7266 – 7269.

[8] T. Ueno, Y. Urano, H. Kojima, T. Nagano, *J. Am. Chem. Soc.* **2006**, *128*, 10640 – 10641.

[9] R. Y. Lai, A. J. Bard, *J. Phys. Chem. B* **2003**, *107*, 5036 – 5042.

[10] R. Ziessel, L. Bonardi, P. Retailleau, G. Ulrich, *J. Org. Chem.* **2006**, *71*, 3093 – 3102.

[11] a) The photogenerated holes in TiO_2 are scavenged by methanol to give the corresponding radical species ($^{\bullet}CH_2OH$) and protons, followed by prompt ET from the radical species to the TiO_2 conduction band:b) O. I. Micic, Y. Zhang, K. R. Cromack, A. D. Trifunac, M. C. Thurnauer, *J. Phys. Chem.* **1993**, *97*, 13284 – 13288.

[12] G. Redmond, D. Fitzmaurice, *J. Phys. Chem.* **1993**, *97*, 1426 – 1430.

[13] P. Gao, D. Gosztola, M. J. Weaver, *J. Phys. Chem.* **1988**, *92*, 7122 – 7130.

[14] a) M. B. J. Roeffaers, G. De Cremer, J. Libeert, R. Ameloot, P. Dedecker, A.-J. Bons, M. Bückins, J. A. Martens, B. F. Sels, D. E. De Vos, J. Hofkens, *Angew. Chem.* **2009**, *121*, 9449 – 9453; *Angew. Chem. Int. Ed.* **2009**, *48*, 9285 – 9289; b) G. De Cremer, M. B. J. Roeffaers, E. Bartholomeeusen, K. Lin, P. Dedecker, P. P. Pescarmona, P. A. Jacobs, D. E. De Vos, J. Hofkens, B. F. Sels, *Angew. Chem.* **2010**, *122*, 920 – 923; *Angew. Chem. Int. Ed.* **2010**, *49*, 908 – 911.

[15] W. Xu, J. S. Kong, P. Chen, *J. Phys. Chem. C* **2009**, *113*, 2393 – 2404.

[16] J. L. Ferry, W. H. Glaze, *J. Phys. Chem. B* **1998**, *102*, 2239 – 2244.

[17] $\langle \tau_{on} \rangle^{-1}$ is independent of [**S**] if $k_2 = k_3$ or $K_2 = 0$.

[18] The influence of the nonuniformity of the laser illumination is negligible because almost the same fluorescence intensity of the bursts was observed for both surfaces. In addition, no apparent change in the photocatalytic activity on the (001) face was observed during photoirradiation, which implies that the bottom surface of the crystal is in direct contact with the bulk solution.

[19] a) T. Ohno, K. Sarukawa, M. Matsumura, *New J. Chem.* **2002**, *26*, 1167 – 1170; b) N. Murakami, Y. Kurihara, T. Tsubota, T. Ohno, *J. Phys. Chem. C* **2009**, *113*, 3062 – 3069; c) C. H. Cho, M. H. Han, D. H. Kim, D. K. Kim, *Mater. Chem. Phys.* **2005**, *92*, 104 – 111; d) N. Wu, J. Wang, D. N. Tafen, H. Wang, J.-G. Zheng, J. P. Lewis, X. Liu, S. S. Leonard, A. Manivannan, *J. Am. Chem. Soc.* **2010**, *132*, 6679 – 6685.

[20] a) X. Han, R. L. Civiello, H. Fang, D. Wu, Q. Gao, P. V. Chaturvedula, J. E. Macor, G. M. Dubowchik, *J. Org. Chem.* **2008**, *73*, 8502 – 8510; b) Y. Gabe, Y. Urano, K. Kikuchi, H. Kojima, T. Nagano, *J. Am. Chem. Soc.* **2004**, *126*, 3357 – 3367.

[21] a) H. G. Yang, C. H. Sun, S. Z. Qiao, J. Zou, G. Liu, S. C. Smith, H. M. Cheng, G. Q. Lu, *Nature* **2008**, *453*, 638 – 641; b) G. Liu, C. Sun, H. G. Yang, S. C. Smith, L. Wang, G. Q. (Max) Lu, H.-M. Cheng, *Chem. Commun.* **2010**, *46*, 755 – 757.